Physica Scripta

RECEIVED
7 March 2023

REVISED
25 April 2023

ACCEPTED FOR PUBLICATION
19 May 2023

PUBLISHED
30 May 2023

PAPER

Structural and magnetic properties of $BaFe_{9.95}Al_2Mg_{0.05}O_{19}$ tuned through sintering temperature

Sana Ullah Asif[1,7,*], **Qasim Ali Ranjha**[2,7], **Ubaid-ur-Rehman Ghori**[3,7], **Basmah H Alshammari**[4,7], **Fahim Ahmed**[5,7,*], **Usman Nawaz**[5,7], **Fatma A Ibrahim**[6,7] **and Mohamed S Hamdy**[6,7]

[1] Key Laboratory of LCR Materials and Devices of Yunnan Province, National Center for International Research on Photoelectric and Energy Materials, School of Materials and Energy, Yunnan University, Kunming 650091, People's Republic of China
[2] Department of Mechanical Engineering, RCET Campus, University of Engineering and Technology, Lahore, Pakistan
[3] Department of Industrial & Manufacturing Engineering (RCET), University of Engineering & Technology, Lahore, Pakistan
[4] Chemistry Department, Faculty of Science, University of Hail, PO Box 2440, Hail 81451, Saudi Arabia
[5] Department of Physics, Division of Science and Technology, University of Education, Lahore, Pakistan
[6] Catalysis Research Group (CRG), Department of Chemistry, College of Science, King Khalid University, PO Box 9004, Abha 61413, Saudi Arabia
[7] All the authors contributed equally.
[*] Author to whom any correspondence should be addressed.

E-mail: sanaullahasif@gmail.com **and** Fahim.ahmed@ue.edu.pk

Keywords: self-biased circulators, magnetic filters, anisotropy field, magnetic anisotropy constant, hexaferrites

Supplementary material for this article is available online

Abstract

The sintering temperature is a key way to tune the structural and magnetic properties of M-type hexaferrites. Here the effect of $BaFe_{9.95}Al_2Mg_{0.05}O_{19}$ M-type hexagonal Ba-hexaferrites, was studied. X-ray diffraction analysis revealed the presence of Fe_2O_3 impurity phases in all samples. The results showed that as the sintering temperature increased, the saturation magnetization (Ms) and remanence ratio (Mr/Ms) initially increased, then decreased at higher temperatures. On the other hand, the coercivity (Hc) and magnetocrystalline anisotropy field (Ha) decreased first, then increased. The average grain size (D) consistently grew between 800–2800 nm with increase in pre-sintering temperature. The optimal magnetic properties of $BaFe_{9.95}Al_2Mg_{0.05}O_{19}$ were achieved at a pre-sintering temperature of 1280 °C, with Ms = 49.94 emu g^{-1}, Hc = 4.99 kOe, Ha = 1.5 kOe, and mB = 9.4097 μB. The findings suggest that magnetic properties of M-type hexagonal strontium ferrite can be significantly enhanced by optimizing the pre-sintering temperature, which has implications for the development of high-performance self-biased circulators, Magnetic filters and other magnetic applications.

1. Introduction

In the recent past, there is an extraordinary boost in scientific research in the field of hexaferrites. Hexaferrites with a crystalline structure known as magneto-plumbite, have become a highly researched topic in recent times [1–5]. On both domestic and industrial levels, hexagonal ferrites have numerous applications, including door magnets, electromagnetic radiation shielding composites/coatings, electric motors, loudspeakers, macro and micro-nutrients for plants, biomedicine, terrestrial and astronomical telecommunications devices, catalysis, radio frequency coils, transverse and longitudinal recording media, transformers, water treatment, hyperthermia fluids, and magnetic resonance imaging (MRI) [6–11]. In the electronics industry, hexagonal ferrites play a crucial role due to their superior dielectric and magnetic characteristics [12]. The magnetic properties of polycrystalline ferrites can vary depending on the synthesis technique, sintering temperature, and the extent of doping. As a result, these materials exhibit excellent magnetic properties [13–15].

M-type hexagonal ferrites, with a magneto-plumbite crystal structure, are considered to be one of the best magnetic materials among its different family members [16]. Its unit cell contains a total of 64 ions, including 24

Fe^{3+}, $2Ba^{2+}$, and $38O^{2-}$ ions. The magnetic materials market, worth $4 billion, is dominated by M-type hexagonal ferrites, which have a 90% share. Approximately 300,000 tons of barium ferrites are produced annually [16]. Researchers are actively exploring its properties such as multiferroic order, magneto-electric coupling, spintronics, magnetic filters and microwave absorption ability due to their moderate chemical and high-temperature stability. These materials have advanced applications in cryogenic electronic switches, quantum memory devices, and electro-caloric refrigeration [17].

Various research studies have been carried out to enhance the hard magnetic properties of M-type hexaferrites by substituting alternative cations for those found in Ba or Fe sites [1, 3, 10, 15, 18]. For instance, the research conducted on the $BaFe_{12-x}Al_xO_{19}$ using a sol-gel self-combustion method showed the coercivity of the substance reached a high of 13.7 kOe. Interestingly, the addition of non-magnetic aluminum ions has been found to be an effective technique for improving the value of Hc in M-type hexaferrites making the potential to enhance the energy density of permanent magnets [19, 20]. A study revealed that the solution auto-combustion method could produce $SrFe_{12-x}Al_xO_{19}$, which had exceptionally high Hc values of approximately 40 kOe [21]. Nevertheless, the Mr value was limited, and non-ferromagnetic phases persisted. Furthermore, results of synthesized $Sr_{1-x}Ca_xFe_{11.8}Mn_{0.1}Zn_{0.1}O_{19}$ revealed that the maximum saturation magnetization of 74.9 emu g^{-1} was achieved [22, 23]. The magnetic properties of M-type hexaferrites can be altered by partially substituting Ba^{2+} and/or Sr^{2+} ions with rare Earth ions including La^{3+}, Nd^{3+}, and Ce^{3+} etc [1–3, 10, 12–15, 24]. In addition to ion substitution, the magnetic properties of M-type hexaferrites can also be influenced by the sintering temperature [25–31].

In this work we have prepared the $BaFe_{9.95}Al_2Mg_{0.05}O_{19}$ hexaferrite and studied the effect of sintering temperature on structure, Morphology and magnetic properties including magnetic anisotropy constant and anisotropic field effects produced in the magnetic material.

2. Experimental work

2.1. Synthesis

In the present study, we have prepared all samples of M-type hexaferrite $BaFe_{9.95}Al_2Mg_{0.05}O_{19}$ through a traditional solid-state reaction method. The starting materials were $BaCO_3$, Al_2O_3, MgO and Fe_2O_3, which were obtained from Sigma Aldrich and had a purity of 99.9%. The ingredients were blended in the stiochiometric proportions required for a reaction. The material was processed for 12 h using a planetary ball mill, in which the ingredients were mixed in nylon jars along with zirconia balls and ethanol as a medium. After the ball milling process, the material was taken out, dried and ground to remove any residual moisture before further processing. The material was subjected to calcination at 1100 °C to eliminate the carbonates, then further processed through ball milling for 6 more hours before being dried and ground again. The material was further reduced to particles less than 100 μm by using a vibration mill. Subsequently, the material was sintered at temperatures between 1220 °C and 1300 °C for a duration of 6 h. The material was shaped into pellets with a diameter of 10 mm and a thickness of 1.1 mm for scanning electron microscopy analysis. To eliminate any PVA binder residue, the pellets were subjected to another sintering process at 900 °C.

2.2. Measurements

The morphology of samples was measured by using the sample pellets by using Scanning Electron Microscopy (SEM) measurements using a HITACHI S-4800 Scanning Electron Microscope. The sample's structural composition was characterized using a Panalytical X'Pert Pro X-Ray diffractometer. Finally, the magnetic properties of the sample were measured at room temperature using a NIM-2000HF magnetic measuring system, which was manufactured in China.

3. Results and discussion

3.1. Structural analysis

Investigating the characteristics of materials structure is a crucial task that can be accomplished using structural analysis [24, 32]. An X-ray diffractometer was utilized to perform XRD measurements of synthesized sample. Figure 1 showed the X-Ray diffraction pattern of $BaFe_{9.95}Al_2Mg_{0.05}O_{19}$ Hexaferrites. The resulting XRD pattern was found to be consistent with JCPDS card #43-0002, which belongs to the hexagonal group p63mmc and space group (194). However, few impurity phases observed due to iron and ruled out at higher sintering temperatures [33, 34].

Reitveld refinement analysis of the synthesized samples of $BaFe_{9.95}Al_2Mg_{0.05}O_{19}$ Hexaferrites were performed to find the lattice parameters of all the samples at different sintering temperatures, which are shown in table 1. The Reitveld refinement process was carried out with the main focus on the iron (Fe) sites. Fe typically

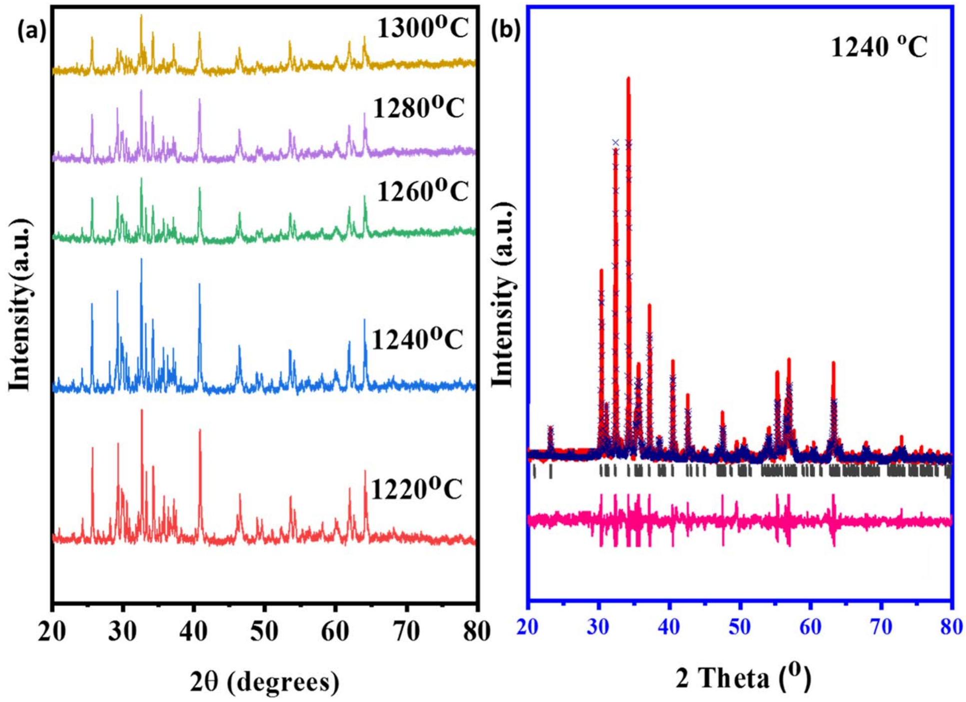

Figure 1. (a) XRD pattern of $BaFe_{9.95}Al_2Mg_{0.05}O_{19}$ at different sintering temperatures. (b) Reitveld refinement profiles of $BaFe_{9.95}Al_2Mg_{0.05}O_{19}$. Red line represents the observed data, while blue+ symbol represents the calculated fitting data. Pink line shows the difference along with black vertical symbols represents the Braggs peak position.

Table 1. Lattice parameters of $BaFe_{9.95}Al_2Mg_{0.05}O_{19}$ Hexaferrites determined from XRD data.

Temperature (°C)	a (Å)	c (Å)	c/a	V (Å)^3	χ^2
1220	5.885	23.1638	3.936075	694.7373	1.074418605
1240	5.8617	23.2091	3.959449	690.5949	1.069605568
1260	5.8589	23.2718	3.972043	691.7992	1.095471236
1280	5.865	23.251	3.964365	692.6209	1.074478649
1300	5.871	23.242	3.95878	693.7701	1.080597015

occupies five different sites, including $4f_1$, which is tetrahedral, 2b, which is trigonal pyramidal, and three octahedral sites − 2a, 12K, and $4f_2$ [19]. Figure 1 showed the XRD patterns of synthesized samples along with refinement profile of selected sample at 1240 °C.

The variations in the intensity of the peaks can be observed as the sintering temperature changes. The results confirm the high-quality crystal structure of the sample. Another crucial parameter to consider is the phase purity along with crystal structure [35]. The XRD results confirmed that the sample was pure throughout all sintering temperatures. The volume of the samples was calculated using the formula given below for hexagonal ferrites.

$$V = 0.866\, a^2 c \tag{1}$$

Figures 2(a)–(b) that the lattice parameters a, c and volume of the sample $BaFe_{9.95}Al_2Mg_{0.05}O_{19}$ varied with sintering temperature. The parameter ‘a’ decreased initially with an increase in sintering temperature, reached its minimum at 1260 °C and then began to increase again. Meanwhile, the parameter ‘c’ increased initially with an increase in sintering temperature, reached its maximum at 1260 °C and then started to decrease again. The changes in these parameters indicated that the lattice initially contracted in the longitudinal direction and then the expansion shifted towards the *c*-axis as the sintering temperature increased. The current observations in the magnetic material system may indicate exciting outcomes. The formation of M-type hexagonal ferrites is also verified as the c/a ratio ranges between 3.9360–3.9720 as shown in table 1 which is less than 3.98 as reported previously [36–39]. Furthermore, the change in lattice parameters happened due to the difference of sintering temperature. Moreover, other microstructural parameters such as average crystallite size D, bulk density d_b, X-ray density d_x, and porosity P of the synthesized samples were also calculated which are given in table 2. Crystallite size (D) was calculated using Scherer method [40, 41] while other parameters like x-ray density (d_x),

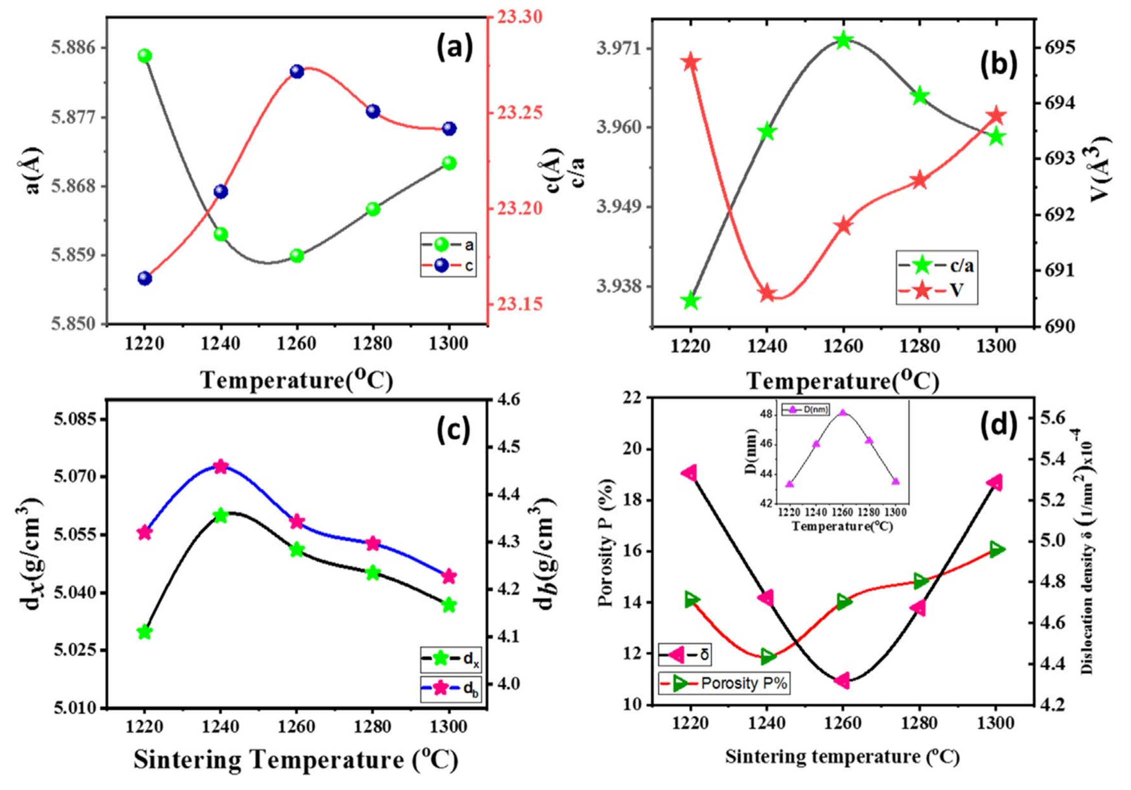

Figure 2. Variations in (a) lattice parameters a and c. (b) c/a ratio and volume (c) X-ray density and Bulk density verses sintering temperature (d) Porosity, Average crystallite size and dislocation density for $BaFe_{9.95}Al_2Mg_{0.05}O_{19}$ at sintering temperatures.

Table 2. Microstructural parameters of $BaFe_{9.95}Al_2Mg_{0.05}O_{19}$ Hexaferrites at different sintering temperatures.

Temperature (°C)	d_x (g cm^{-3})	d_b (g cm^{-3})	D (nm)	P (%)	δ (1/nm2) × 10^{-4}
1220	5.029701	4.32	43.302	14.11757	5.33
1240	5.059871	4.39	46.012	11.88315	4.72
1260	5.051062	4.56	48.12	14.02223	4.32
1280	5.04507	4.69	46.25	14.83829	4.67
1300	5.036713	4.79	43.491	16.07656	5.29

Bulk density (d_b) and Porosity (P) were calculated using formulas given below [42–44].

$$D = \frac{K\lambda}{\beta Cos\theta} \tag{2}$$

$$d_x = \frac{ZM_w}{N_A V} \tag{3}$$

$$d_b = \frac{m}{\pi r^2 h} \tag{4}$$

$$P = \left(1 - \frac{d_b}{d_x}\right) \times 100 \tag{5}$$

Where k = 0.9, λ = 1.5409 Å, Z = 2 and β, θ, M_w, N_A, are FWHM, Peak position, Molar weight, Avogadro's number respectively while m, r, h is Mass, radius and length of the pallet respectively. In the end, to check the vacant spaces present in the material, dislocation density (δ) was calculated using the formula given below [42].

$$\delta = \frac{1}{D^2} \tag{6}$$

Where D is the average crystallite size. All the parameters are displayed in table 2.

The concept of dislocation density (δ) plays an important role in understanding the distribution of voids or empty spaces among small agglomerated crystallites in ceramic materials. This concept is particularly useful in

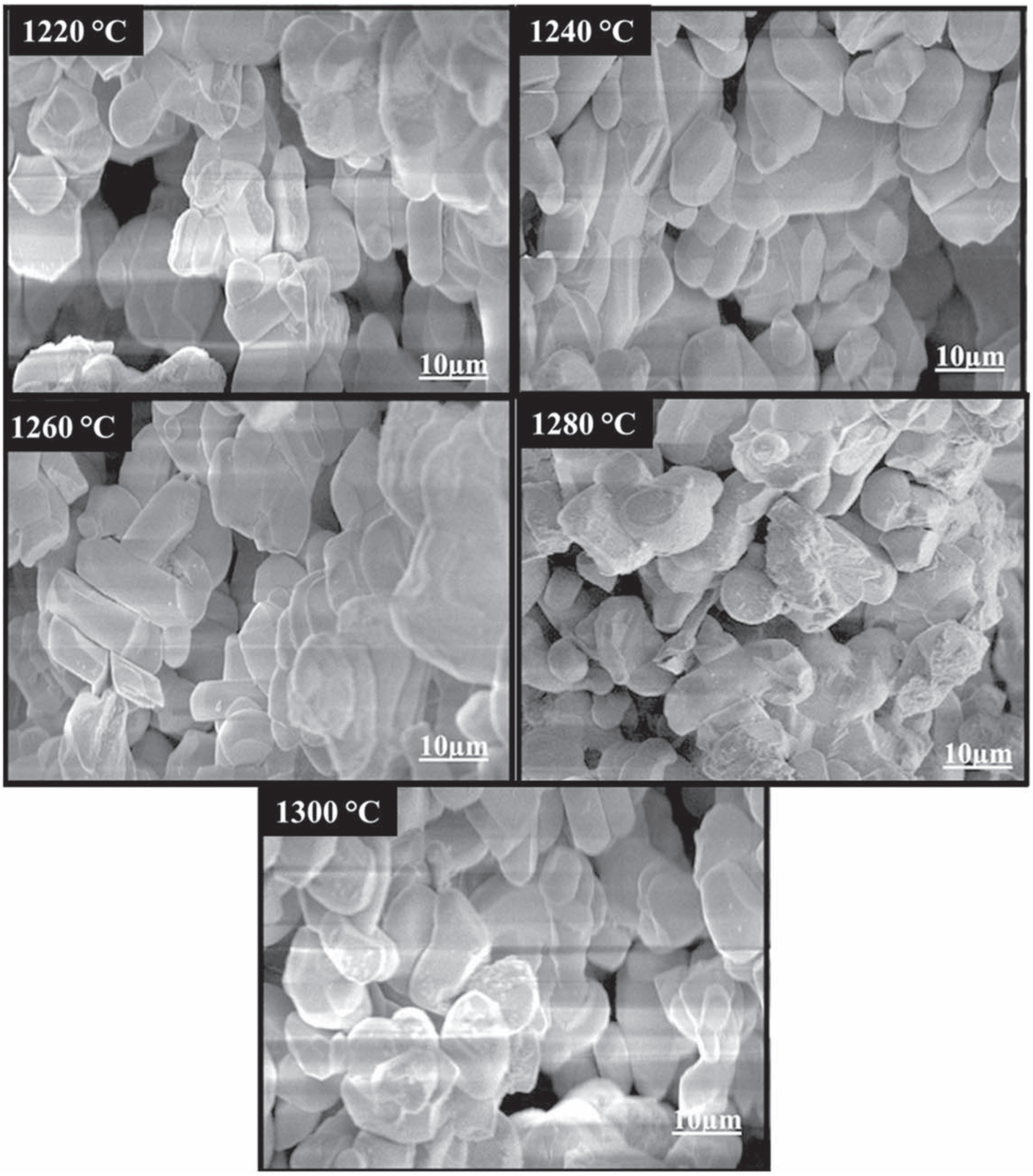

Figure 3. Scanning electron micrograph of $BaFe_{9.95}Al_2Mg_{0.05}O_{19}$ hexaferrites at different sintering temperatures.

evaluating the sintering behavior of these materials. In this context, figure 2(c) presents the relationship between the two densities (d_x and d_b) and the sintering temperature. As observed from the plot, an increase in sintering temperature lead to an increase in the values of both densities (d_x and d_b) upto 1240 °C after that start decreasing. On the other hand, figure 3(d) depicts the evolution of porosity, Average crystallite size and dislocation density with respect to sintering temperature. It can be seen that the porosity of the sample remained in the range 11%–16%. This behavior is in accordance with the expectations, as a higher sintering temperature reduces the voids in the material and makes it denser [45]. Therefore, this information sheds light on the influence of sintering temperature on the microstructure and porosity of ceramic materials and can be used to optimize the processing conditions for these materials. The greater values of X-ray density suggest the presence of pores in the samples while changes in dislocation density (δ) and porosity (P) could be well linked to the change in oxide vacancies as well. Overall such changes in micro parameters are linked to the variation in magnetic characteristics of materials [28, 46, 47].

3.2. Morphological analysis

Scanning electron microscopy was conducted on samples of synthesized $BaFe_{9.95}Al_2Mg_{0.05}O_{19}$ hexaferrites to determine the presence of secondary phases and the formation of shape. The results showed that there were no

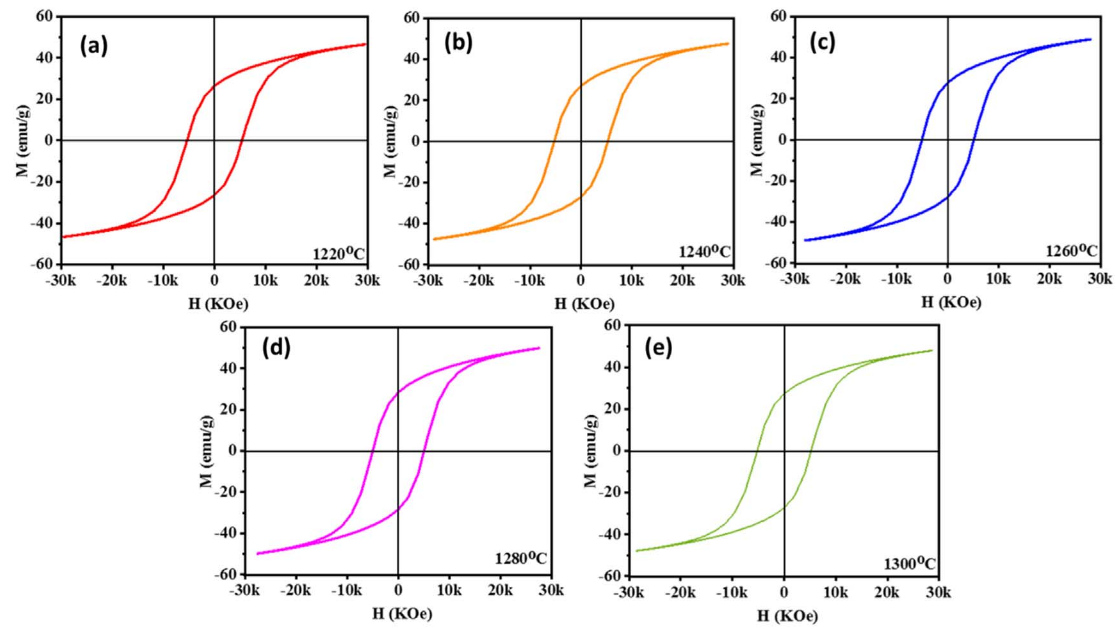

Figure 4. Hysteresis loops of $BaFe_{9.95}Al_2Mg_{0.05}O_{19}$ at (a) 1220 °C (b) 1240 °C (c) 1260 °C (d) 1280 °C (e) 1300 °C.

Table 3. Magnetic parameters saturation magnetization (Ms), remanence magnetization (Mr), Coercivity (Hc), Mr/Ms Ratio, Magnetic anisotropy constant and magnetic moment per formula unit and anisotropy field (H_a) were obtained by analysis of M–H loops of $BaFe_{9.95}Al_2Mg_{0.05}O_{19}$.

Temperature (°C)	M_s (emu g^{-1})	M_r(emu g^{-1})	M_r/M_s	H_c (KOe)	K(erg/kOe)	m_B (μ_B)	Ha(Oe)
1220	46.920	26.410	0.5628	5.350	0.04925	8.8391	1671.72
1240	47.640	27.120	0.5692	5.308	0.04962	8.9747	1658.60
1260	49.066	28.014	0.5709	5.225	0.05030	9.2433	1632.66
1280	49.949	28.590	0.5723	4.993	0.04893	9.4097	1560.17
1300	48.503	27.550	0.5680	5.170	0.04920	9.1373	1615.47

secondary phases in the material and that the hexagonal shape of the particles was evident in the micrographs. The SEM images in figure 2 was also confirmed that the samples were homogenously and uniformly distributed [18, 30]. Pores present in the images showed the removal of PVA binder. The introduction of dopants did not result in significant changes in the grain size, suggesting that doping may affect the shape rather than the size of the hexaferrites. Overall, the morphological images confirmed the successful formation of pure hexaferrites. The grain size was observed between 800 to 2800 nm.

3.3. VSM results

The magnetic properties of $BaFe_{9.95}Al_2Mg_{0.05}O_{19}$ were measured between applied magnetic fields of ±30 kOe and the hysteresis loop of the material was shown in figures 4(a)–(e). Table 3 provided the calculated values of magnetic parameters such as magnetic saturation (Ms), coercivity (Hc), remanence (Mr), crystalline isotropic constant (K), magnetic moment per formula unit and anisotropy field (Ha).

The figure 5(a) displayed the relationship between the Ms and Mr of the synthesized samples with sintering temperature. The figure 5(b) represnets the relationship of Hc and Mr/Ms ratio with sintering temperature. From table 3 it is clear that value of Mr/Ms is above 0.5 indicating the formation of M-type hexaferrites [39, 48].

The first sample had a coercivity of 5.35 kOe and magnetic saturation of 46.92 emu g^{-1} when it was sintered at 1220 °C. The results were comparable to previously reported results for M-type hexaferrites [25, 49]. The slight differences in results with changing sintering temperature were attributed to variations in the synthesis process. As the sintering temperature increased, both Ms and Mr values changed and reached a maximum at 1280 °C with values of 49.949 emu g^{-1} and 28.59 emu g^{-1} respectively. After that, both values decreased. Coercivity Hc, on the other hand, decreased to a minimum at 1280 °C and then started increasing again, as shown in the figure 5(b). The variation in the values of Ms and Hc with respect to sintering temperature is connected to the decline in the strength of the octahedral and tetrahedral super exchange mechanism described by Gorter's model [48]. However, in some cases, the reduction in magnetic properties may be related to the

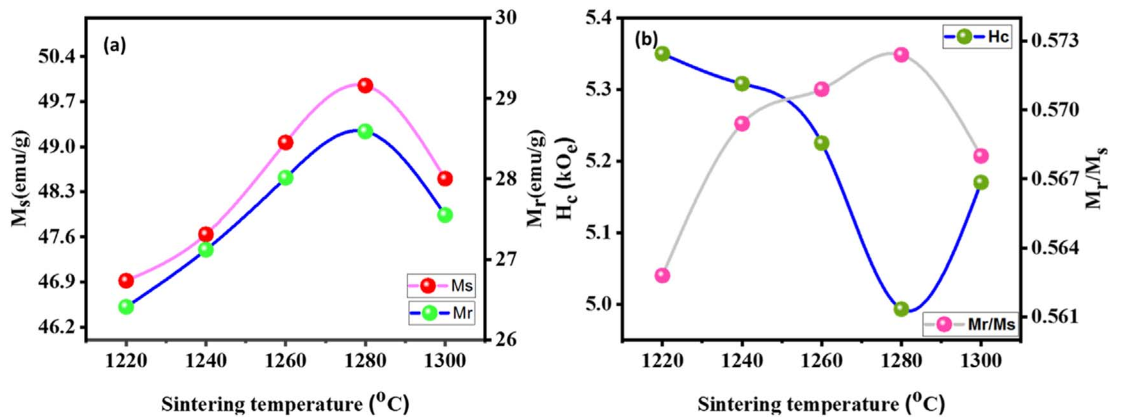

Figure 5. (a) Variation in magnetic saturation and magnetic remanence against sintering temperature. (b) Coercivity and Mr/Ms ratio with sintering temperature.

suppression or weakening of the crystalline phase at elevated temperatures. Heat treatments are commonly used to modify the microstructure of solid materials. Prolonged heat treatments result in the diffusion of atoms within the solid material, leading to the redistribution of atoms and the reduction of dislocations. This reduction in dislocations, in turn, decreases the distance between magnetic ions and reduces the magnetic effects that result from spin–orbit and spin-spin coupling. As a result, heat treatments can have a significant impact on the magnetic properties of materials. Additionally, the presence of single-domain structure in the synthesized materials is confirmed by the observation of a Mr/Ms ratio greater than 0.5 [30, 50].

These findings make the material highly useful in magnetic applications, such as recording media, magnetic filters, and spintronics. For determining the magnetic moment per formula unit in terms of Bohr's magnetron the following formula is used [18].

$$m_B = \frac{Ms \times Mr}{5585} \tag{7}$$

The obtained parameters were shown in table 3. Magnetocrystalline anisotropy constant K was also calculated and given in table 3. The trends of k in agreement with the Ms and Hc value which is another key factor which influence the properties is the charge compensation mechanism that arises due to the difference of sintering temperature. Another important key factor to describe the magnetic properties of M-type Hexaferrites are the anisotropy field(Ha) and anisotropy Parameter (B) which are calculated using the following formulas [15, 51].

$$H_a = \frac{2K}{\mu_o M_s} \tag{8}$$

$$B = \frac{4K^2}{15{\mu_o}^2{M_s}^2} \tag{9}$$

Where μ_o is the permeability of free space and K is magnetocrystalline anisotropy constant. Parameter (B) arises due to magnetocrystalline anisotropy resistance on domain wall rotation.

The calculated value of 'K' and 'Ha' are given in table 3. As shown in table 3 and figures 6(a)–(b), both Hc and Ha firstly decreases then start increasing with increasing sintering temperature. Both 'Hc' and 'Ha' becomes minimum at 1280 °C. The literature [52] suggests that as Ms decreases, Hc increases, and the effect of Ms on Hc is predominant when the variations between D and K is minimal. The highest value of Ms at sintering temperature of 1280 °C (49.949 emu g^{-1}) results in the lowest Hc (4.993 kOe). The strength of magnetic field (Hc) is inversely proportional to magnetic saturation (Ms), with a major effect when differences in grain size and magnetic anisotropy constant K are not significant. The highest Ms value of 49.949 emu g^{-1} at a pre-sintering temperature of 1280 °C results in the lowest Hc. The magnetic field anisotropy (Ha) and d decreased with pre-sintering temperature, while porosity negatively affects Ha. However, in this work, there is a decreasing trend in Ha initially, than increased at 1300 °C due to the increasing BaM content and plate-like shape of the BaM particles with high aspect ratio at higher sintering temperatures [53, 54].

4. Conclusions

The present work focuses on the synthesis of M-type Ba-hexaferrite $BaFe_{9.95}Al_2Mg_{0.05}O_{19}$ using the solid-state reaction method. The study examines the impact of pre-sintering temperature on the phase, microstructure,

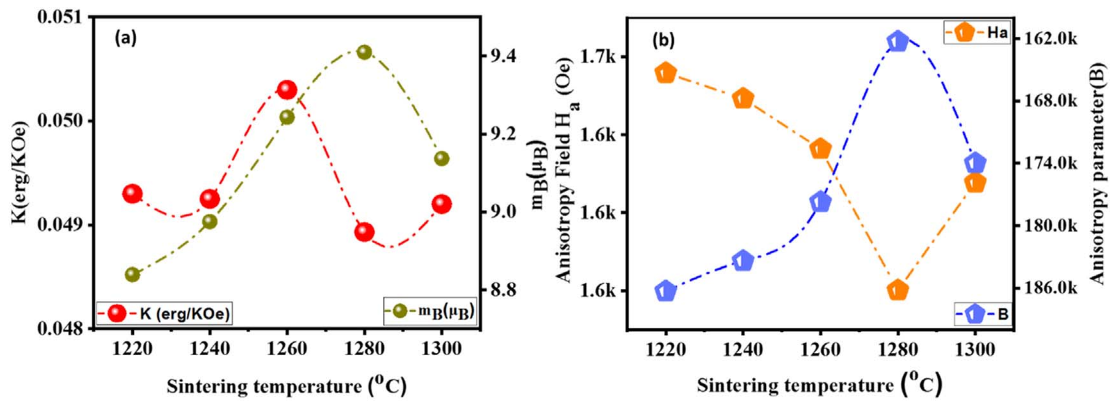

Figure 6. (a) Magnetic anisotropy constant(K) and magnetic moment per formula unit(m_B) (b) anisotropy field (H_a) and anisotropy parameter(B) versus sintering temperature.

and magnetic properties of the samples using XRD, SEM, and VSM. The results show that all samples contain Fe_2O_3 phases, whose content decreases with increasing pre-sintering temperature. The saturation magnetization, and remanence ratio increase initially and then decrease with increasing pre-sintering temperature. Similarly, the coercivity and magnetocrystalline anisotropy field decrease initially and then increase with increasing pre-sintering temperature. The best magnetic properties were observed in samples pre-sintered at 1280 °C, with Ms = 49.94 emu g^{-1}, Mr/Ms = 0.57, Hc = 4.99 kOe, Ha = 1.5 kOe. All samples showed high Mr/Ms, making them potential candidates for use in magnetic applications.

Acknowledgments

The authors would like to thank the Deanship of Scientific Research at King Khalid University for funding this work through large group Research Project under grant number RGP2/236/44.

Data availability statement

All data that support the findings of this study are included within the article (and any supplementary files).

Author contributions

All the authors contributed equally in this work. U.N. synthesized the material. All the authors analyzed the data. The manuscript was written through the contributions of all authors. The work is part of thesis of U.N. All authors have given approval to the final version of the manuscript.

Declaration

The authors declare that they have no known competing financial interests or personal relationships that could have appeared to influence the work reported in this paper.

ORCID iDs

Sana Ullah Asif https://orcid.org/0000-0002-1521-5747
Qasim Ali Ranjha https://orcid.org/0000-0001-9071-2893
Basmah H Alshammari https://orcid.org/0000-0002-5876-3700
Fahim Ahmed https://orcid.org/0000-0001-5530-9492
Mohamed S Hamdy https://orcid.org/0000-0002-7234-4924

References

[1] Kumar H, Singh A and Rana K 2023 Effect of substitution on the dielectric and magnetic properties of BaFe12O19 *An Introduction to Hard Ferrites: From Fundamentals to Practical Applications* **142** 66–92

[2] Jasrotia R, Suman A V, Godara S K, Sharma S, Kirti R K, Puri P and Kumar G 2023 Hard ferrites for permanent magnets *An Introduction to Hard Ferrites: From Fundamentals to Practical Applications* **142** 121–51
[3] Khongorzul B, Jargalan N, Tsogbadrakh N, Odkhuu D, Trukhanov S, Trukhanov A and Sangaa D 2023 Correlation of the crystal features, magnetic parameters, and electronic structure of Bi-substituted BaFe12-xBixO19 hexaferrites: Theoretical background *Ceram. Int.* **49** (10) 15492–9
[4] Martínez-Pérez J, Sánchez-De Jesús F, Cortés-Escobedo C and Bolarín-Miró A 2023 Magnetocapacitance on the transition fields in Ni2 + doped Y-type hexaferrite Ba0. 6Sr1. 4Co2Fe11AlO22 obtained by high-energy ball milling *Ceram. Int.* **49** 2663–9
[5] Younus S, Murtaza G, Aloufi N M and Somaily H 2022 Structural, dielectric, and magnetic properties of Pr–Cr co-doped PrxBa1-xCryFe12-yO19 barium hexaferrites *Ceram. Int.* **48** 31041–53
[6] Harris V G 2022 Societal benefits of ferrites: historical, scientific, and commercial breakthroughs *Modern Ferrites: Basic Principles, Processing and Properties* **1** 9–20
[7] No, S., Mandatory Courses* S. no. *Sriperumbudur TK-602 117 Regulation–2018 B. Tech Biotechnology* 8
[8] Socoliuc V, Avdeev M, Kuncser V, Turcu R, Tombácz E and Vekas L 2022 Ferrofluids and bio-ferrofluids: Looking back and stepping forward *Nanoscale* **14** 4786–886
[9] Thakur P, Gahlawat N, Punia P, Kharbanda S, Ravelo B and Thakur A 2022 Cobalt nanoferrites: a review on synthesis, characterization, and applications *J. Supercond. Nov. Magn.* **35** 2639–69
[10] Verma R, Chauhan A and Kumar R 2023 Applications of hard ferrites in memory devices *An Introduction to Hard Ferrites: From Fundamentals to Practical Applications* **142** 185–206
[11] Zhang J 2023 A low reflection absorbent conductive carbon black-coated BaZn2Fe16O27 composite covering X and Ku bands *J. Mater. Sci., Mater. Electron.* **34** 158
[12] Basfer N and Almaghamsi H 2023 Investigation of magnetic, dielectric and electrical modulus of Ce3+ doped cobalt–magnesium ferrite nanoparticles *J. Rare Earths*
[13] Badiger H, Matteppanavar S and Hegde B 2023 Structural, electrical and magnetic properties of low dimensional Pr-doped Co-Zn ferrite nanoparticles *J. Supercond. Nov. Magn.* 1–10
[14] Jing X, Guo M, Li Z, Qin C, Chen Z, Li Z and Gong H 2023 Study on structure and magnetic properties of rare Earth doped cobalt ferrite: the influence mechanism of different substitution positions *Ceram. Int.*
[15] Lu S, Liu Y, Yin Q, Chen J, Wu J and Li J Enhanced magnetic properties of Sr0. 7Ce0. 3Fe11. 7Zn0. 3O19 by tuning pre-sintering temperature *J. Alloys Compd.* **2023** 168833
[16] Mohammed I, Mohammed J and Srivastava A K 2023 Recent progress in hexagonal ferrites based composites for microwave absorption *Cryst. Res. Technol.* **58** (3) 22002002200200
[17] Lukianov M, Ahmed A, Bush A, Prokhorov A, Anzin V, Gorshunov B and Alyabyeva L 2021 In Terahertz spectroscopy of lead-substituted barium hexaferrites Ba1-xPbxFe12O19 *Journal of Physics: Conf. Series* IOP Publishing **1984** 1–3012013
[18] Asif S U, Ranjha Q A, Ghori U-u-R, Nisa M, Ahmad M S, Bukhari M, Jabeen N, Hussain A, Hassan N and Ahmed F 2023 Exploring the structural and magnetic trends in Ba0.9Sm0.1Fe12−xAlxO19 M-type Hexaferrites *Phys. Scr.* **98** 015836
[19] Trusov L A, Gorbachev E A, Lebedev V A, Sleptsova A E, Roslyakov I V, Kozlyakova E S, Vasiliev A V, Dinnebier R E, Jansen M and Kazin P E 2018 Ca–Al double-substituted strontium hexaferrites with giant coercivity *Chem. Commun.* **54** 479–82
[20] Han G, Sui R, Yu Y, Wang L, Li M, Li J, Liu H and Yang W 2021 Structure and magnetic properties of the porous Al-substituted barium hexaferrites *J. Magn. Magn. Mater.* **528** 167824
[21] Gorbachev E A, Trusov L A, Sleptsova A E, Kozlyakova E S, Alyabyeva L N, Yegiyan S R, Prokhorov A S, Lebedev V A, Roslyakov I V and Vasiliev A V 2020 Hexaferrite materials displaying ultra-high coercivity and sub-terahertz ferromagnetic resonance frequencies *Mater. Today* **32** 13–8
[22] Moon K-S and Kang Y-M 2016 Structural and magnetic properties of Ca-Mn-Zn-substituted M-type Sr-hexaferrites *J. Eur. Ceram. Soc.* **36** 3383–9
[23] Jiang X, Jia H, Wu C, Yu Z, Luo H, Guo R, Li Z, Jiang Y, Nie J and Lan Z 2020 Cation distribution and magnetic characteristics of textured BaFe12-xScxO19 hexaferrites: experimental and theoretical evaluations *J. Alloys Compd.* **835** 155202
[24] Wagner D V, Kareva K V, Zhuravlev V A, Dotsenko O A and Minin R V 2023 Investigation of BaFe12O19 Hexaferrites manufactured by various synthesis methods using a developed pulsed magnetometer *Inventions* **8** 26
[25] Makhdoom A, Ranjha Q A, Raza M A, Raza B, Mazhar M E, Rao K A, Ahmed F, Asif S U, Khan M W and Nisa M 2021 Structural and magnetic variations in Ba0. 5Sr0. 5Fe9Ce1Al2O19 hexaferrites at different sintering temperatures *Phys. Scr.* **96** 125865
[26] Martirosyan K S, Galstyan E, Hossain S M, Wang Y-J and Litvinov D 2011 Barium hexaferrite nanoparticles: Synthesis and magnetic properties *Materials Science and Engineering: B* **176** 8–13
[27] Pandu R, Yadav K L, Kumar A, Reddy P R and Gupta A V S S K S 2010 Effect of sintering temperature on structural and electrical properties of BiFeO3 multiferroics *Indian J. of Engineering and Materials Sciences* **17** 481–5
[28] Awan M Q, Ahmad J, Waheed A, Gillani S A R, Ahmed F, Asif S U, Mazhar M E and Anwar S 2021 Facile synthesis and characterizations of Co2+ doped Bi0.8Ba0.2FeO3 nano-crystalline multiferroic ceramics *Phys. Scr.* **96** 105805
[29] Sharma P, Verma A, Sidhu R K and Pandey O P 2003 Influence of Nd3+ and Sm3+ substitution on the magnetic properties of strontium ferrite sintered magnets *J. Alloys Compd.* **361** 257–64
[30] Makhdoom A R *et al* Structural and magnetic variations in $Ba_{0.5}Sr_{0.5}Fe_9Ce_1Al_2O_{19}$ hexaferrites at different sintering temperatures *Phys. Scr.* 2021 **96** 125865
[31] El Shater R E, El-Ghazzawy E H and El-Nimr M K 2018 Study of the sintering temperature and the sintering time period effects on the structural and magnetic properties of M-type hexaferrite BaFe12O19 *J. Alloys Compd.* **739** 327–34
[32] Asif S U, Wang J, Qian Y, Gao D, Bashir R, Bilal M K, Ahmad J, Awan M Q and Hu W 2020 Phonon vibrations and photoluminescence emissions and their correlations with the electrical properties in Er3+ doped Bi3YO6 oxide-ion conductors *Solid State Ionics* **344** 115092
[33] Roy D, Choudhari Y, Rewatkar K, Kokode N and Borikar D 2021 In investigation of structural and dielectric properties of Co-Zr doped Barium M-type Hexaferrites *Journal of Physics: Conf. Series* IOP Publishing: **1913** 1–5012056
[34] Makhdoom A, Ahmed F, Ghori U-u-R, Ranjha Q A, Rao K A, Javed A, Mazhar M E, Bukhari M, Maqsood A and Asif S U 2022 Tuning magnetic properties in the Ce–Al Co-substituted M-type BaSr (6: 4) hexaferrites *J. Mater. Sci., Mater. Electron.* **33** 7266–74
[35] Godara S K, Kaur V, Malhi P S, Ahmed J, Alshehri S M, Singh M, Verma S, Singh C, Maji P K and Kumar P 2022 Sol-gel auto-combustion synthesis of double metal-doped barium hexaferrite nanoparticles for permanent magnet applications *J. Solid State Chem.* **312** 123215
[36] Wu C, Li J, Lan Z, Yu Z, Jiang X, Guo R, Luo Q and Sun K 2020 Crystallographically textured Ba0. 8La0. 2Fe11. 8-xCu0. 2O19-δ hexaferrites with narrow FMR linewidth *Ceram. Int.* **46** 8719–24

[37] Shezad M, Liu X, Feng S, Kan X, Wang W, Liu C, Shehzad T J and Rehman K M U 2020 Characterizations analysis of magneto-structural transitions in Ce-Co doped SrM based nano Sr1−xCexFe12−xCoxO19 hexaferrite crystallites prepared by ceramic route *J. Magn. Magn. Mater.* **497** 166013
[38] Liu C *et al* Investigations of Ce-Zn co-substitution on crystal structure and ferrimagnetic properties of M-type strontium hexaferrites Sr1-xCexFe12-xZnxO19 compounds *J. Alloys Compd.* 2019 **785** 452–9
[39] Rehman K M U, Liu X, Li M, Jiang S, Wu Y, Zhang C, Liu C, Meng X and Li H 2017 Synthesization and magnetic properties of Ba1−xYxFe12O19 hexaferrites prepared by solid-state reaction method *J. Magn. Magn. Mater.* **426** 183–7
[40] Rani N, Chahal S, Chauhan A S, Kumar P, Shukla R and Singh S 2019 X-ray analysis of MgO nanoparticles by modified Scherer's Williamson-Hall and size-strain method *Mater. Today Proc.* **12** 543–8
[41] Bindu P and Thomas S 2014 Estimation of lattice strain in ZnO nanoparticles: x-ray peak profile analysis *Journal of Theoretical and Applied Physics* **8** 123–34
[42] Vlassak J 2004 A model for chemical–mechanical polishing of a material surface based on contact mechanics *J. Mech. Phys. Solids* **52** 847–73
[43] Barakat M M, Bakeer D E-S and Sakr A-H 2020 Structural, magnetic properties and electron paramagnetic resonance for BaFe12-xHgxO19 hexaferrite nanoparticles prepared by co-precipitation method *Journal of Taibah University for Science* **14** 640–52
[44] Li L-Z, Sokolov A, Yu C-J, Li Q-F, Qian K and Harris V G 2021 Effects of Y–Co co-substitution on the structural and magnetic properties of M-type strontium hexaferrites *Ceram. Int.* **47** 25514–9
[45] Lange F 1984 Sinterability of agglomerated powders *J. Am. Ceram. Soc.* **67** 83–9
[46] Deraz N and Alarifi A 2012 Processing and evaluation of alumina doped nickel ferrite nano-particles *Int. J. Electrochem. Sci.* **7** 4585–95
[47] Asif S U *et al* Effect of Dy-Co on physical and magnetic properties of X-type hexaferrites (Ba2−xDyxCu2Fe28−yCoyO46) *Chin. J. Phys.* 2019 **61** 47–54
[48] Shezad M, Liu X, Feng S, Kan X, Wang W, Liu C, Shehzad T J and Rehman K M U 2020 Characterizations analysis of magneto-structural transitions in Ce-Co doped SrM based nano Sr1− xCexFe12− xCoxO19 hexaferrite crystallites prepared by ceramic route *J. Magn. Magn. Mater.* **497** 166013
[49] Kumar N P, Chary K A, Sumana B, Rao K S, Suresh M, Raja M M and Srinivas A 2019 Investigation of sintering methodologies and its influence on magnetic and electric properties of $NiFe_2O_4$: a comparative study *Mater. Res. Express* **6** 086112
[50] Makhdoom A R *et al* 2022 Tuning magnetic properties in the Ce–Al Co-substituted M-type BaSr (6:4) hexaferrites *J. Mater. Sci., Mater. Electron.* **33** 7266–74
[51] You J-H, Kim H-J and Yoo S-I 2017 Preparation of strontium W-type hexaferrites in a low oxygen pressure and their magnetic properties *J. Alloys. Compd.* **695** 3011–7
[52] Patel C D, Dhruv P N, Meena S S, Singh C, Kavita S, Ellouze M and Jotania R B 2020 Influence of Co4+-Ca2+ substitution on structural, microstructure, magnetic, electrical and impedance characteristics of M-type barium–strontium hexagonal ferrites *Ceram. Int.* **46** 24816–30
[53] Lee J, Lee E J, Hwang T-Y, Kim J and Choa Y-H 2020 Anisotropic characteristics and improved magnetic performance of Ca–La–Co-substituted strontium hexaferrite nanomagnets *Sci. Rep.* **10** 15929
[54] Hashhash A, Hassen A, Baleidy W S and Refai H S 2021 Impact of rare-Earth ions on the physical properties of hexaferrites Ba0.5Sr0.5RE0.6Fe11.4O19, (RE = La, Yb, Sm, Gd, Er, Eu, and Dy) *J. Alloys Compd.* **873** 159812